Developmental Cell *11*, 375–385, September, 2006 ©2006 Elsevier Inc. DOI 10.1016/j.devcel.2006.07.014

Transiently Reorganized Microtubules Are Essential for Zippering during Dorsal Closure in *Drosophila melanogaster*

Ferenc Jankovics[1] and Damian Brunner[1,*]
[1] Cell Biology and Biophysics Unit
European Molecular Biology Laboratory
Meyerhofstrasse 1
69117 Heidelberg
Germany

Summary

There is emerging evidence that microtubules in nondividing cells can be employed to remodel the intracellular space. Here, we demonstrate an essential role for microtubules in dorsal closure, which occurs toward the end of *Drosophila melanogaster* embryogenesis. Dorsal closure is a morphogenetic process similar to wound healing, whereby a gap in the epithelium is closed through the coordinated action of different cell types. Surprisingly, this complex process requires microtubule function exclusively in epithelial cells and only for the last step, the zippering, which seals the gap. Preceding zippering, the epithelial microtubules reorganize to attain an unusual spatial distribution, which we describe with subcellular resolution in the intact, living organism. We provide a clearly defined example where cells of a developing organism transiently reorganize their microtubules to fulfill a specialized morphogenetic task.

Introduction

Microtubules (MTs) are polar tubes that constantly switch between phases of growth and shrinkage (Desai and Mitchison, 1997). They execute diverse, conserved functions such as chromosome segregation in mitosis or serving as tracks for motor proteins and their cargo (Karsenti and Vernos, 2001; Welte, 2004). MTs can also exert forces to position organelles or cellular structures (Dogterom et al., 2005; Grill et al., 2001; Tran et al., 2001). In nondividing cells, MTs are believed to predominantly promote housekeeping functions such as organelle positioning/shaping and vesicle trafficking, which occur in every eukaryotic cell. There is however, increasing evidence that MTs are also employed to perform specialized tasks. This appears to be important particularly during the development of multicellular organisms when cells need to change their intracellular organization in response to the signals orchestrating morphogenesis. A classical example of specialized MT function is polarization of the developing *Drosophila melanogaster* oocyte where MT-mediated, localized delivery of oskar mRNA defines the position of the posterior pole (Riechmann and Ephrussi, 2001). More recently, it was shown that in developing muscle cells, MTs serve as a scaffold for sarcomere formation and that in the growth cones of neuronal axons, MT function is required to change growth direction (Buck and Zheng, 2002; Pizon et al., 2005). Transient MT deployment may also occur in response to environmental challenges that provoke a change in the behavior of fully differentiated cells. For example, MTs are reorganized in cultured epithelial cells if artificial wounds are scratched into a monolayer of cells (Etienne-Manneville, 2004). The reason for this MT reorganization is not fully understood but it is believed to support cell migration toward the wound.

A common feature of specialized MT function is that it is preceded by spatial MT rearrangements (Pizon et al., 2005; Riechmann and Ephrussi, 2001). Establishment and subsequent maintenance of a new MT distribution requires altered spatial control of MT dynamics. This involves local positioning of the MT minus ends and regional control of the polymerization and depolymerization dynamics of the plus ends (Akhmanova and Hoogenraad, 2005; Dammermann et al., 2003). Bundling and sliding processes can also contribute to MT organization (Carazo-Salas et al., 2005). Often, the MT minus ends focus into a single site, the centrosome, but there are examples where they associate with the nuclear envelope, the cell membrane, or are distributed in the cytoplasm (Dammermann et al., 2003).

To date, the functional analysis of spatial MT organization in nondividing cells of multicellular organisms was carried out using isolated, cultured cells. Here, we performed such analysis in vivo, by using intact, living dorsal closure (DC) stage embryos of the fruit fly *Drosophila melanogaster*. DC is a morphogenetic process where an eye-shaped gap in the dorsal epithelium that is occupied by amnioserosa cells is closed. DC is orchestrated by the Jun kinase, the dpp, and the wg signaling pathways (Jacinto et al., 2002; Kaltschmidt et al., 2002). These control two major events that bring about DC. First, the two lateral epithelial cell layers approach each other by moving dorsally, which we here term convergence. Secondly, the epithelial cells of each layer sequentially meet and connect to each other at the anterior- and posterior-most ends of the opening, a process called zippering. Convergence requires the apical constriction of the amnioserosa cells, which generates a force that pulls the lateral epithelial cell sheets toward the midline (Kiehart et al., 2000). At the same time, the epithelial cells change shape and elongate along their dorsal/ventral (D/V) axis. In addition, the dorsal-most row of epithelial cells (DME cells) polarize parallel to the D/V axis, excluding proteins of the cell-cell adhesion complexes and accumulating actin and myosin II at their dorsal surface (Kaltschmidt et al., 2002). This allows contraction of the dorsal side of the DME cells, which further narrows the epithelial gap. DME cells also execute zippering by forming cellular protrusions, lamellipodia and filopodia, at their dorsal membrane. The protrusions provide the initial contacts for connecting cells, and by interdigitating, they promote their association (Harden et al., 1996; Jacinto et al., 2000).

DC is interesting to study due to its similarities to wound-healing processes and because it shows several important cellular behaviors such as cooperative cell movement, tissue force generation, and cell shape

*Correspondence: damian.brunner@embl.de

changes (Hutson et al., 2003; Jacinto et al., 2001, 2002; Kiehart et al., 2000). While much is known about the requirements of the actin cytoskeleton during DC, the role of the MTs has not been addressed. Previous observations in fixed DC-stage embryos showed that MTs are aligned parallel to the D/V cell axis in epithelial cells (Kaltschmidt et al., 2002). Here, we have used real-time fluorescence imaging to describe the spatial distribution and the dynamic behavior of these MTs and to study their role during DC. We describe, to our knowledge, a novel spatial MT distribution, which is established in the cells of the converging epithelium. Thereby, multiple, antiparallel MTs form bundles at the apical cell cortex that align with the D/V cell axis. Although bundles are stable, individual MTs remain highly dynamic. MTs are not anchored at centrosomes but are associated individually with the apical cell cortex. Surprisingly, solely these MTs are essential for DC whereas MTs in all other relevant cells are dispensable. We demonstrate that epithelial MTs control exclusively a single essential step, the final zippering, and show evidence that this may be linked to a role in promoting cell-protrusion formation. Our results provide the first detailed in vivo analysis of spatial MT organization and function in nondividing cells of an intact multicellular organism and reveal a surprisingly specific role for the MTs during a complex morphogenetic process.

Results

Epithelial MT Organization during DC

Previous immunofluorescence experiments showed a parallel MT arrangement in epithelial cells during DC (Kaltschmidt et al., 2002). To obtain a picture of the dynamic behavior of these MTs, we performed real-time imaging of living stage 14–15 embryos expressing GFP-tagged α-tubulin driven by the ectoderm specific 69B-Gal4 driver. At the onset of DC (stage 14), MTs were detectable throughout epithelial cells. Mainly due to limitations in z axis resolution, we were unable to follow the entire length of single MTs and therefore resolve details of their distribution. As DC proceeded, MTs began forming stable arrays that aligned parallel to the D/V cell axis (Figures 1A–1D and Movie S1) and were restricted to the apical cell cortex (Figures 1A and 1B). MT rearrangement was initiated first in DME cells and after a delay of about 1 hr in the remaining epithelial cells (Figures 1C and 1D and Movie S2). MT alignment improved during the entire DC process, coinciding with the gradual elongation and the apical/basal thinning of the cells (Figure 1A and 1B and Movie S2). Once formed, the MT arrays were stable and moved only very little within cells (Figure 1E and Movie S2).

At the zippering stage, the cells at the leading edges of the epithelium extend dynamic cell protrusions, lamellipodia and filopodia, which can be visualized by expression of a CFP-tagged variant of actin (Actin-ECFP). In embryos simultaneously expressing Actin-ECFP and GFP-tubulin, we observed that dynamic MTs intruded into lamellipodia and filopodia (Figure 1F and Movie S3). Thereby, MTs frequently spanned the entire length of growing and shrinking filopodia.

Approximately 30 min after cells from opposite sides of the embryo had merged, MT arrays disassembled, and MTs acquired a distribution similar to that observed prior to DC (Figure 1G and Movie S4). Disassembly coincided with a shortening of the elongated epithelial cells. The observed formation of stable MT arrays is thus restricted to DC.

During DC MTs Are Required Exclusively for Zippering

The formation and disappearance of MT arrays tightly correlate with the onset and completion of DC, indicating that MT rearrangement is important for this process. To investigate this possibility, we eliminated MTs after DC onset by injecting embryos with the MT depolymerizing drug colcemid. The embryos expressed Moe-GFP or Arm-EGFP to outline the cells (Edwards et al., 1997; McCartney et al., 2001). We followed DC 30 min after colcemid injection when MTs appeared completely depolymerized. Epithelial cells converged toward the dorsal midline with a similar velocity as in control embryos and amnioserosa cells displayed normal apical constriction (Figures 2A–2D and Movie S5). This suggests that MTs are dispensable for convergence of the lateral epithelial cell sheets. In contrast to convergence, the zippering process was strongly affected by the absence of MTs. In wild-type embryos, the epithelial gap displays an ellipsoidal shape during the entire zippering process because convergence occurs concomitantly with zippering at the anterior and posterior ends (Figure 2E and Movie S6). In colcemid-treated embryos, the dorsal opening became abnormally narrow (Figure 2F and Movie S6). This is because convergence continued normally while zippering was almost absent (Figures 2G, 2H, and 2J). The embryos arrested development without completing DC (Figure 2F). UV-induced colcemid inactivation resulted in a rapid resumption of zippering and the completion of DC (Figures 2I and 2J and Movie S6). We calculated the fractional contribution of zippering (f_z) to the velocity of closure by using previously published equations (Hutson et al., 2003). f_z was 28% in wild-type control embryos but dropped to 4% in colcemid-treated embryos. Our results show that MT function is essential for zippering.

In colcemid-treated embryos, epithelial cells elongated less than in the wild-type and eventually acquired irregular cell borders (Figure 3A). As zippering DME cells are polarized along the D/V cell axis, we tested whether the abnormal cell shape was linked to abnormal D/V polarity (Morel and Arias, 2004). This can be monitored because actin is strongly enriched at the dorsal cell cortex in DME cells, whereas proteins such as Frizzled (Fz) or Discs-large (Dlg) are excluded (Kaltschmidt et al., 2002). We found that the localization of GFP-tagged forms of these proteins in DME cells of colcemid-treated embryos was similar to wild-type (Figures 3B and 3C). MTs therefore are not required to maintain D/V cell polarity.

Zippering Is Mediated by Epithelial MTs

In our drug-induced MT-depletion experiments, we eliminated MTs in all embryonic cells. The observed effects on zippering and cell shape could therefore be an indirect consequence of defects caused by the absence of MTs in nonepithelial cells. To clarify this point, we eliminated MTs specifically in epithelial cells by

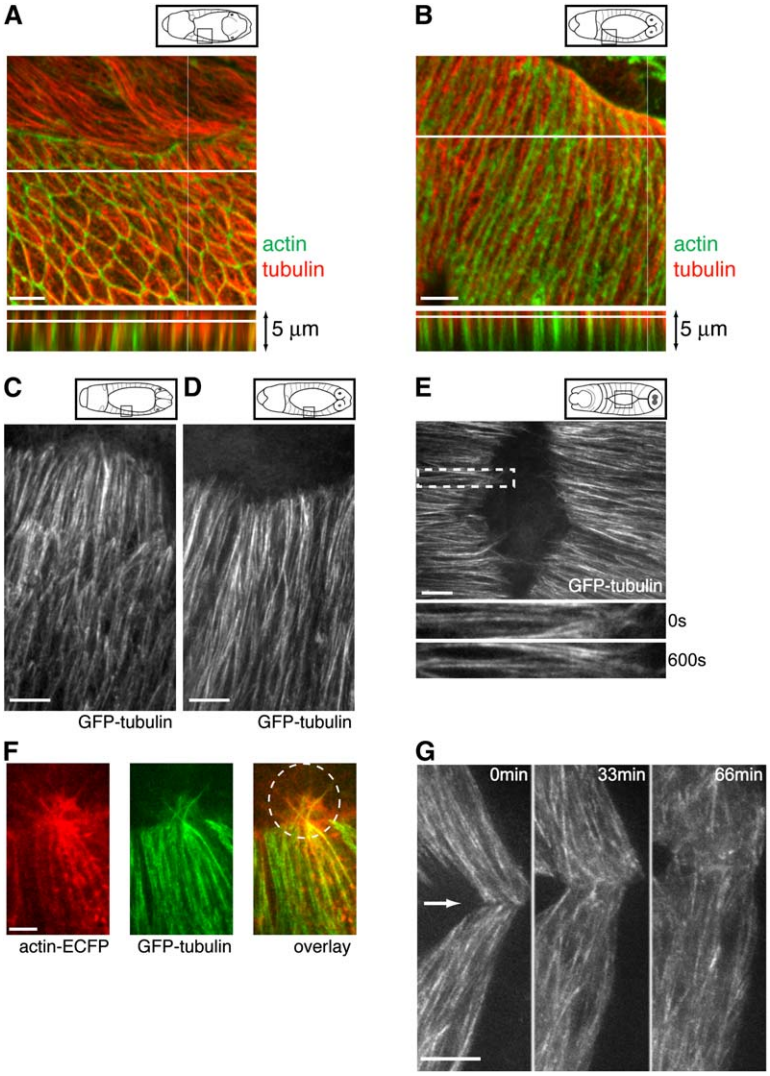

Figure 1. MT Distribution during DC

In all figures, dorsal is up unless stated differently. Scale bars are 5 μm. All frames are full projections of confocal sections covering at least the entire MT-containing cell region. (A and B) Immunofluorescence experiment with fixed wild-type embryos using anti-tubulin antibody to stain MTs (red) and phalloidin to stain actin and outline the cells (green). The bottom shows cross-sections parallel to the A/P cell axis. (A) Embryo at the onset of DC. (B) Zippering-stage embryo. Note the more apical tubulin in the cross-section as compared to (A). (C and D) Images of a living embryo showing MT array formation in approximately three rows of GFP-tubulin expressing epithelial cells. (C) Living embryo at the onset of DC. DME cells have rearranged their MTs. (D) One hour later, MTs have also rearranged in the remaining epithelium. (E) Frames taken from movie sequence showing GFP-tubulin-expressing DME cells in an embryo toward the end of DC. The first frame shows a dorsal overview. The boxed area is enlarged in the bottom frames showing two time points. MT arrays in the cell body (left half) do not change much, but MTs at the leading edge (on the right) are dynamic. (F) DME cells expressing GFP-tubulin and Actin-ECFP in a living embryo toward the end of DC. MTs penetrate into the protrusions (dotted area). (G) Movie sequence of DME cells expressing GFP-tubulin in engrailed expressing stripes of cells. In the first frame, the DME cells from opposite sides have just met at the dorsal midline (arrow), and MT arrays are still intact.

ectopic expression of the MT-severing protein Spastin. In muscle cells, this was previously shown to cause MT disassembly (Sherwood et al., 2004). We used the engrailed-Gal4 driver to restrict expression of an EGFP tagged form of Spastin under UAS promotor control (enGal4;UAS-Spas-EGFP) to alternating stripes of epithelial cells. The stripes encompass four rows of cells, which alternate with seven to eight rows of "wild-type" cells that do not express the transgene. We first immunolabeled MTs in fixed DC-stage embryos expressing enGal4;UAS-Spas-EGFP with an anti-tubulin antibody. At the onset of DC, the MT network had completely disappeared from enGal4;UAS-Spas-EGFP-expressing cells, while cells in the nonexpressing neighboring stripes contained the normal MT arrays (Figure 4A). We imaged living enGal4;UAS-Spas-EGFP embryos that also expressed Moe-GFP to visualize the cell borders. The early stages of embryogenesis and DC were not affected by the Spastin-mediated absence of MTs. All DME cells moved synchronously toward the midline with similar velocity compared to the wild-type (Figure 2C and Movie S7). Only when zippering began could we detect abnormalities. While wild-type stripes of cells zippered normally, the zippering process halted as soon as Spastin-expressing cell stripes met at the midline, showing that the epithelial MT arrays are indeed essential for zippering (Figure 4B and Movie S7). The zippering block was eventually overcome as the continued convergence of the epithelial cell sheets brought the adjacent stripes of wild-type cells close enough to enable their interaction. This resulted in resumption of zippering through the wild-type cell stripe until the next Spastin-expressing cells again halted the process. Once Spastin-expressing cells were forced together, the weakening Moe-GFP signal in between them indicated that they also slowly managed to merge. This allowed the embryos to complete DC, but the entire process was strongly delayed with f_z dropping to 7% similarly to colcemid-treated embryos (Figure 2J).

As in colcemid-treated embryos, the Spastin-expressing cells displayed abnormal shapes, suggesting that the effect of MT disruption on cell shape is cell autonomous. We also checked the D/V polarity markers (e.g., actin, Dlg) and found that they localize normally in Spastin-expressing cells, confirming that D/V polarity is not affected by the absence of MTs (Figures 4C–4F).

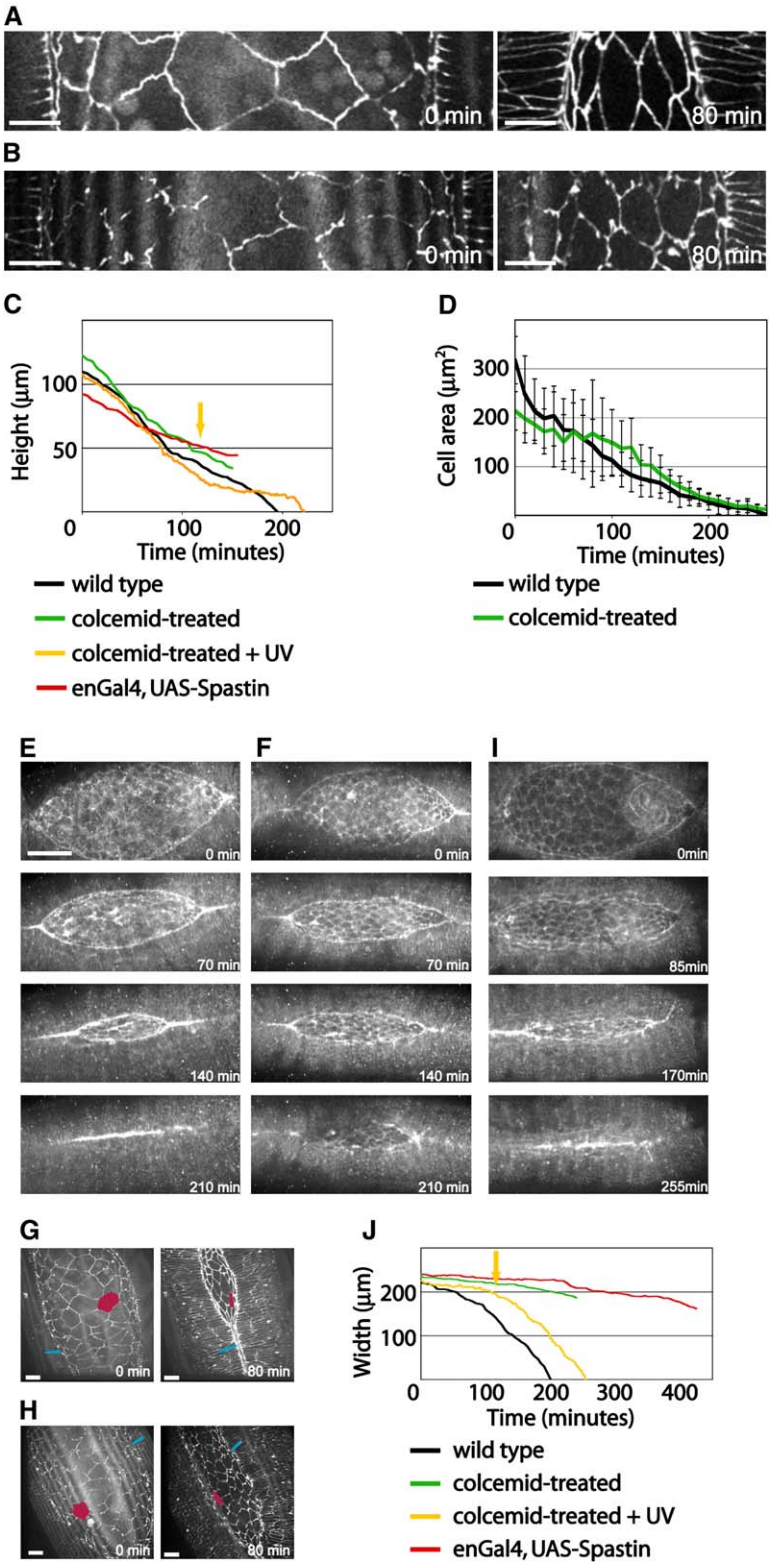

Figure 2. MTs Are Required for Zippering

(A and B) Frames from movie sequences of arm-GFP-expressing embryos. Dorsal view. Scale bars are 10 μm. (A) Buffer-injected control embryo. (B) Colcemid-injected embryo.

(C) Graph showing the kinetics of convergence in a buffer-injected control embryo, two colcemid-injected embryos (one with subsequent UV inactivation [arrow] of colcemid) and an en-Gal4/+;Spas-EGFP/+-expressing embryo. "Height" is the maximal distance between the converging cell layers.

(D) Quantification of amnioserosa cell contraction in a buffer-injected control embryo and a colcemid-injected embryo with standard deviation.

(E, F, and I) Movie sequences of Moe-GFP-expressing embryos. Dorsal view. Scale bar is 50 μm. (E) Buffer-injected control embryo. (F) Colcemid-injected embryo. (I) Colcemid-injected embryo, UV-irradiated for 30 s 116 min after injection.

(G and H) Frames taken from movie sequence of Arm-GFP-expressing embryos. Dorsal view. Individual amnioserosa (red) and DME cells (blue) are highlighted. Scale bars are 10 μm. (G) Buffer-injected control embryo. (H) Colcemid-injected embryo.

(J) Graph showing zippering kinetics of the epithelial cell sheets in a in a buffer-injected control embryo, two colcemid-injected embryos (one with subsequent UV inactivation [arrow] of colcemid) and an en-Gal4/+;/UAS-Spas-EGFP/+-expressing embryo. "Width" represents the maximal distance between zippering ends.

Cell Protrusions Are Dependent on MTs

Zippering requires the function of lamellipodia and filopodia. These are dynamic cellular protrusions extending at the dorsal side of DME cells. Their formation depends on the activities of actin and the actin-organizing machinery (Woolner et al., 2005; Jacinto et al., 2000). Our observation of MTs growing into these protrusions indicated a possible link between MTs and protrusion formation. To test this, we visualized protrusions in a subset of cells by expressing UAS promoter controlled Actin-EGFP with the en-GAL4 driver and performed real-time imaging. In embryos, injected with colcemid after the

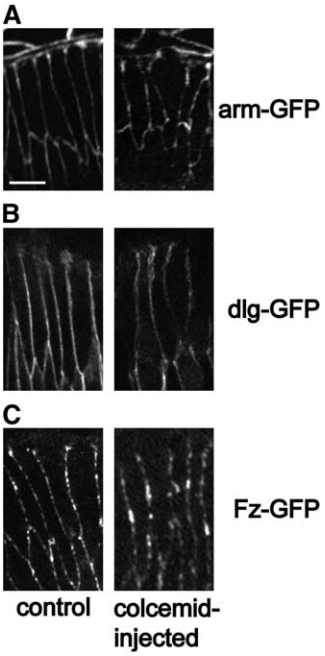

Figure 3. MTs Are Not Required for D/V Polarization

(A–C) DME cells of a buffer-injected control embryo and colcemid-injected embryos at the zippering stage. Scale bar is 5 μm. (A) Embryo expressing Arm-GFP. (B) Embryo expressing Dlg-GFP. (C) Embryo expressing Fz-GFP.

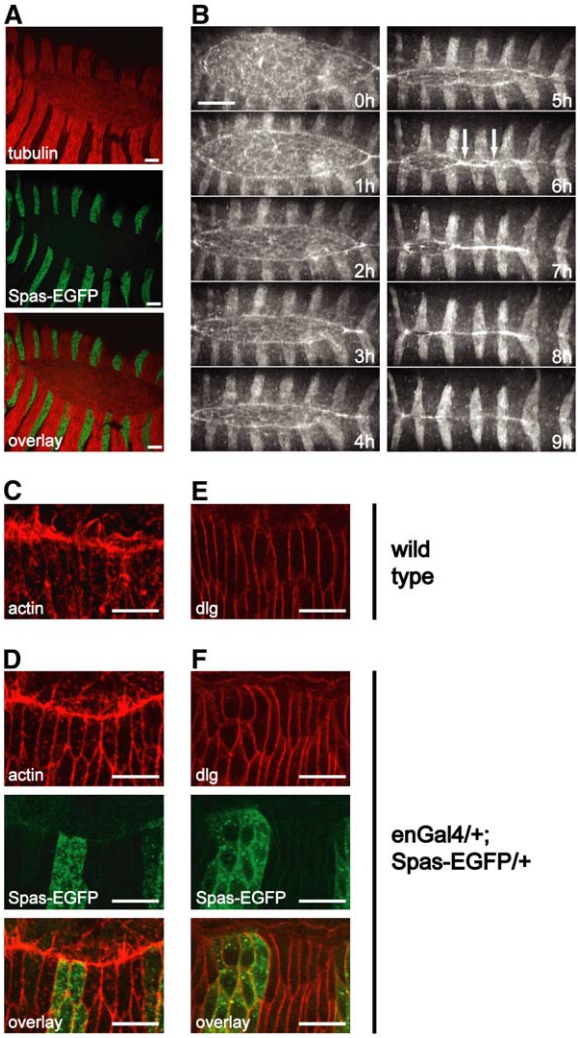

Figure 4. Epithelial MTs Are Required for Zippering

Scale bars are 10 μm except for (B). (A) Immunofluorescence staining with anti-tubulin antibody (red) of an embryo expressing Spas-EGFP in engrailed expressing stripes of cells. Dorsal view. (B) Movie sequence showing the kinetics of the closure process in an embryo ubiquitously expressing Moe-GFP and expressing Spas-EGFP in engrailed expressing stripes of cells. White arrows point to regions where wild-type cell stripes have fused, whereas neighboring Spas-EGFP expressing stripes have not. Scale bar is 50 μm. (C and D) Phalloidin staining of actin in zippering stage DME cells. Dorsal view. (C) Wild-type embryo. (D) Embryo expressing Spas-EGFP (green) in engrailed expressing cell stripes. (E and F) Immunofluorescence staining with anti-Dlg antibody (red) of zippering stage embryos. (E) Wild-type embryo. (F) Embryo expressing Spas-EGFP (green) in engrailed expressing cell stripes.

onset of DC, protrusion formation was considerably affected (Figures 5A and 5B and Movies S8 and S9). Filopodia number was reduced from 1.5 ± 0.4/min in the wild-type to 0.4 ± 0.2/min in the drug-treated embryos, although their average length was not greatly affected (4.6 ± 1.6 μm in wild-type [n = 70] versus 4.0 ± 1.8 μm in colcemid-treated embryos [n = 55]). Lamellipodia were less dynamic, strongly reduced in size and covering less than 5 μm^2 on average as compared to more than 10 μm^2 in the wild-type (Figure 5E and Movies S8 and S9). UV-induced inactivation of colcemid resulted in an immediate normalization of filopodia number and lamellipodia size (Figures 5C and 5E and Movie S9). MT function is thus essential for proper protrusion formation in DME cells.

We also followed protrusion formation in embryos coexpressing Actin-EGFP and EGFP-tagged Spastin under en-GAL4 control, selectively eliminating MTs in Actin-EGFP-expressing stripes of epithelial cells. The effect on these cells was similar to that in colcemid-injected embryos (Figure 5D and Movie S10). The number of filopodia (0.5 ± 0.3/min) but not their average length (4.2 ± 2.0 μm [n = 44]) was reduced, and the size of the lamellipodia decreased to below 5 μm^2 (Figure 5E). MTs therefore control protrusion formation in a cell-autonomous manner.

Arrays Are Bundles of Dynamic, Antiparallel MTs

Our findings suggest that epithelial cells reorganize their MTs to perform a specific morphogenetic task. To better understand this MT reorganization process, we further investigated the nature of the observed MT arrays by visualizing the growth dynamics of individual MTs. We therefore constructed EYFP- and GFP-tagged versions of *Drosophila* EB1, which, like its homologs in other organisms, was shown to be an excellent marker of growing MT plus ends (Akhmanova and Hoogenraad, 2005; Rogers et al., 2002). Coexpression of EB1-EYFP and GFP-tubulin revealed multiple EB1-EYFP dots all along the epithelial MT arrays, suggesting that arrays consist of multiple MTs (Figures 6A and 6B). Real-time imaging showed that these dots were highly dynamic. At the onset of DC, prior to MT array formation, they moved randomly throughout the cytoplasm (Figure 6C and Movie S11). Thereafter, EB1-GFP movement rapidly became bidirectional occurring parallel to the D/V cell axis

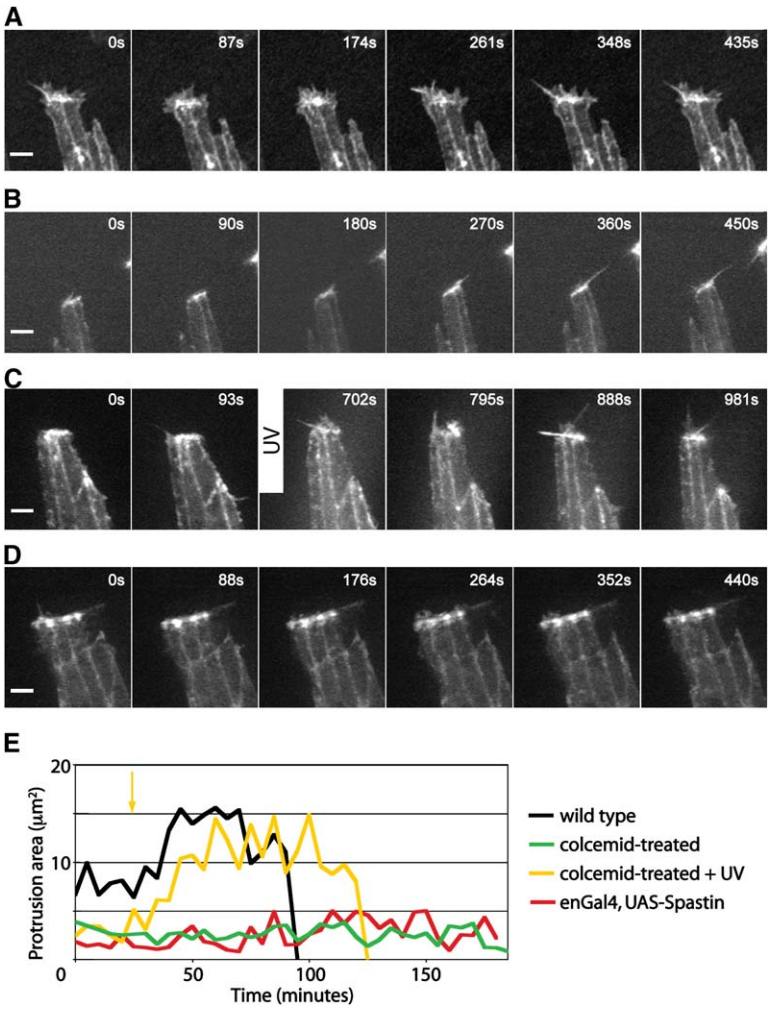

Figure 5. MTs Promote Protrusion Formation

(A–D) Movie sequences showing DME cell protrusion dynamics in embryos expressing Actin-EGFP in engrailed expressing cell stripes. Scale bars are 5 μm. (A) Buffer-injected control embryo. (B) Colcemid-injected embryo. (C) Colcemid-injected embryo, irradiated for 30 s with UV as indicated. (D) Embryo expressing Spas-EGFP in Engrailed-expressing cell stripes.

(E) Graph showing the average surface area covered by lamellipodia in buffer-injected control embryos, colcemid-injected embryos, colcemid-injected embryos with subsequent UV-mediated colcemid inactivation (arrow), and Spas-EGFP-expressing embryos.

(Movie S12). Projection images of consecutive timepoints visualized EB1-GFP tracks and thus the MT arrays (Figure 6D). Kymographs produced from such tracks showed that EB1-GFP dots moved bidirectionally along the majority of tracks (Figure 6E). The velocity was on average 8.0 ± 1.6 μm/min (n = 57) in dorsal and 7.4 ± 2.4 μm/min (n = 50) in ventral directions. This is in the range of the displacement velocity measured for growing MT plus ends in *Drosophila* Schneider cells (Mennella et al., 2005). Our data show that the stable MT arrays appearing during DC are bundles of multiple, dynamic MTs with antiparallel orientation.

In fission yeast, where similar bundling of antiparallel MTs occurs, bundled MTs also slide along each other (Carazo-Salas et al., 2005). To test whether such sliding occurred in epithelial MT bundles, we performed iFRAP experiments with GFP-tubulin-expressing embryos. We partially photobleached the MTs in an area covering several DME cells, leaving only a thin stripe of fluorescence, perpendicular to the MT bundles. If MT sliding occurred, we would expect this stripe to broaden. However, this was not the case as the GFP-tubulin stripe displayed an even, gradual loss of fluorescence ($t_{1/2}$ = 66 s, n = 7) (Figures 6F and 6G and Figure S2). Similar results were obtained with FRAP experiments (Figure S1). This shows that MTs do not slide inside the cell and confirms that within the seemingly stable bundles individual MTs are dynamic.

MT Minus Ends Do Not Localize to a Centrosome

Using EB1-GFP kymographs, we monitored the de novo appearance of EB1-GFP dots and found Gaussian distributions that peaked in the cell center with a bias toward the dorsal side for dots that moved ventrally and vice versa (Figure 7A). EB1-GFP dots usually moved all the way to the cell ends where they rapidly disappeared (Movie S12). As EB1-GFP accumulates at growing MT plus ends (Rogers et al., 2002), its appearance marks MT growth initiation. Unfortunately, it was impossible to discriminate whether this was the consequence of new MT nucleation, which would reveal the position of MT minus ends, or of regrowth following the rescue of a depolymerizing MT.

To determine the position of MT minus ends, we visualized centrosomes by immunolabeling Pericentrin-like protein (d-plp), a constitutive component of centrioles (Martinez-Campos et al., 2004). Each epithelial cell contained two randomly positioned d-plp dots suggesting that the cells do not contain a single classical centrosome (Figure 7B). Real-time imaging of zippering-stage embryos expressing the PACT domain of d-plp fused to GFP (GFP-PACT) showed that except for occasional

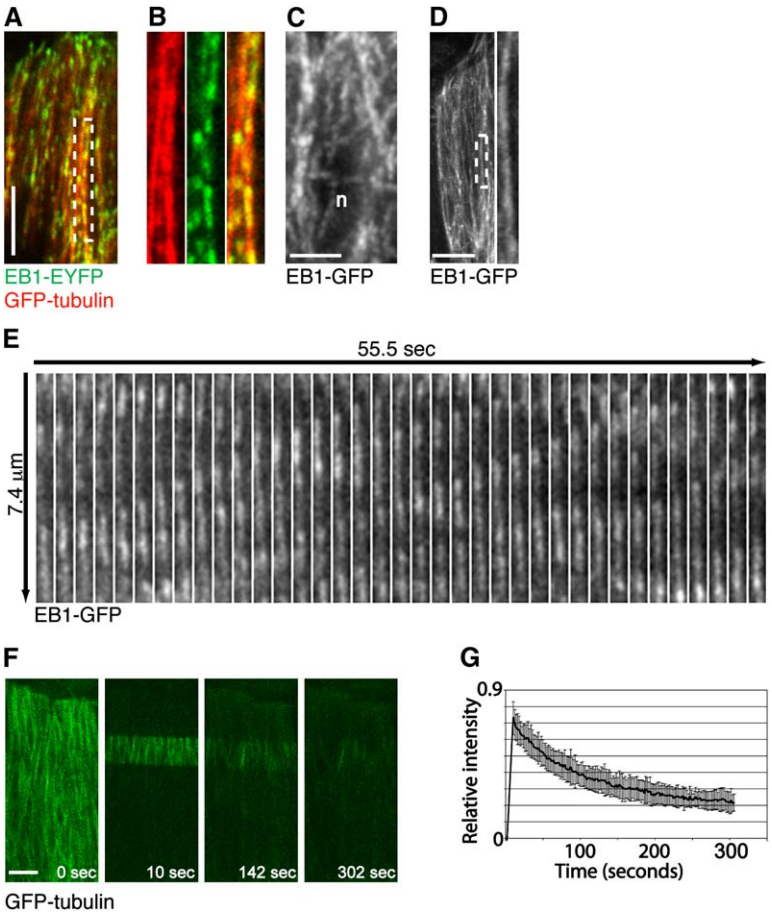

Figure 6. MT Dynamics in DME Cells

Scale bars are 5 μm except for (C). (A) DME cells of a zippering-stage embryo expressing GFP-tubulin (red) to visualize the MTs and EB1-EYFP. (B) Magnification of the boxed area in (A) showing GFP-tubulin (red) and EB1-EYFP dots (green) and an overlay. (C) Projection of six consecutive time points of a movie sequence of an EB1-GFP-expressing epithelial cell before DC (n, nucleus). Scale bar is 2 μm. (D) Projection of 20 consecutive time points of a movie sequence of EB1-GFP-expressing DME cells during DC. The enlarged boxed area highlights a single track formed by moving EB1-GFP dots. (E) Kymograph of the boxed region in (D). (F) Movie sequence showing GFP-tubulin turnover and the absence of MT sliding in a typical iFRAP experiment. (G) Graph showing the fluorescence loss of unbleached GFP-tubulin in iFRAP experiments. The curve represents the averaged single exponential decays of seven individual experiments. Error bars show standard deviation.

short pauses, the two GFP-PACT particles moved independently and mostly parallel to the D/V cell axis with up to 12 μm/min (Figures 7C and 7D and Movie S13). Similar results were obtained with embryos expressing GFP-tagged forms of AuroraA and Centrosmin, both of which were previously shown to localize to centrosomes in mitosis (data not shown) (Berdnik and Knoblich, 2002; Megraw et al., 2002). The fact that cells possess more MT bundles than centrioles shows that at most two of the bundles can contain centriole-associated MT minus ends. However, the fast velocity of the centrioles means that associated MTs should show fast sliding, a process we could not detect in our iFRAP experiments. We conclude that the majority, or maybe all, of the bundled MTs are not anchored with their minus ends at centrosomal structures.

MT Minus Ends Associate with the Apical Cell Cortex

While we have performed immunolabeling of several components of the γ-tubulin complex that normally cap MT minus ends and could therefore reveal their position (e.g., γ-tubulin, Dgrip84, Dgrip91, Dgrip163, Dgrip75, Dgrip128), these experiments did not produce any distinct, detectable signal above background levels (data not shown). In an alternative approach, we performed MT regrowth experiments. MTs were depleted from stage 15 embryos expressing GFP-tubulin or EB1-GFP by injecting the MT-depolymerizing drug colcemid. Thirty minutes after colcemid injection, the GFP-tubulin expressing embryos displayed an almost complete loss of MTs (Figure 7E). Similarly, in colcemid-injected EB1-GFP expressing embryos, we could only detect a few, mostly static EB1-GFP dots (Figure 7F). To induce MT regrowth, we inactivated the colcemid with a 2–5 s exposure to UV light (Wilkie and Davis, 2001). Immediately following UV treatment, we observed multiple, simultaneous nucleation events, in GFP-tubulin and EB1-GFP-expressing embryos. Nucleation occurred mostly in the apical region of the cells, but nucleation sites were randomly distributed within this region. This suggests that MT minus ends associate with the apical cell cortex at random positions (Figure 7G). Growing MTs usually did not leave the apical cell region, suggesting that they were also associated with the apical cell cortex. However, within this region, they displayed a criss-cross orientation. (Figures 7E–7G and Movie S14). In the EB1-GFP-expressing embryos, single isolated MTs as well as small MT asters were visible. The MTs disappeared again after about a minute probably due to diffusion of active drug from neighboring regions. To find out if the initial criss-cross arrangement of the regrowing MTs would fully transform back into the oriented bundles, we improved drug elimination by extending UV treatment to 15 s, which allowed us to follow longer MT growth periods. In embryos expressing GFP-tubulin, MT bundles with the correct orientation and appearance reformed within 10 min (Figure 7H). Likewise, in EB1-GFP-expressing embryos, the initial criss-cross movement of the EB1-GFP dots turned into the normal bidirectional movement along

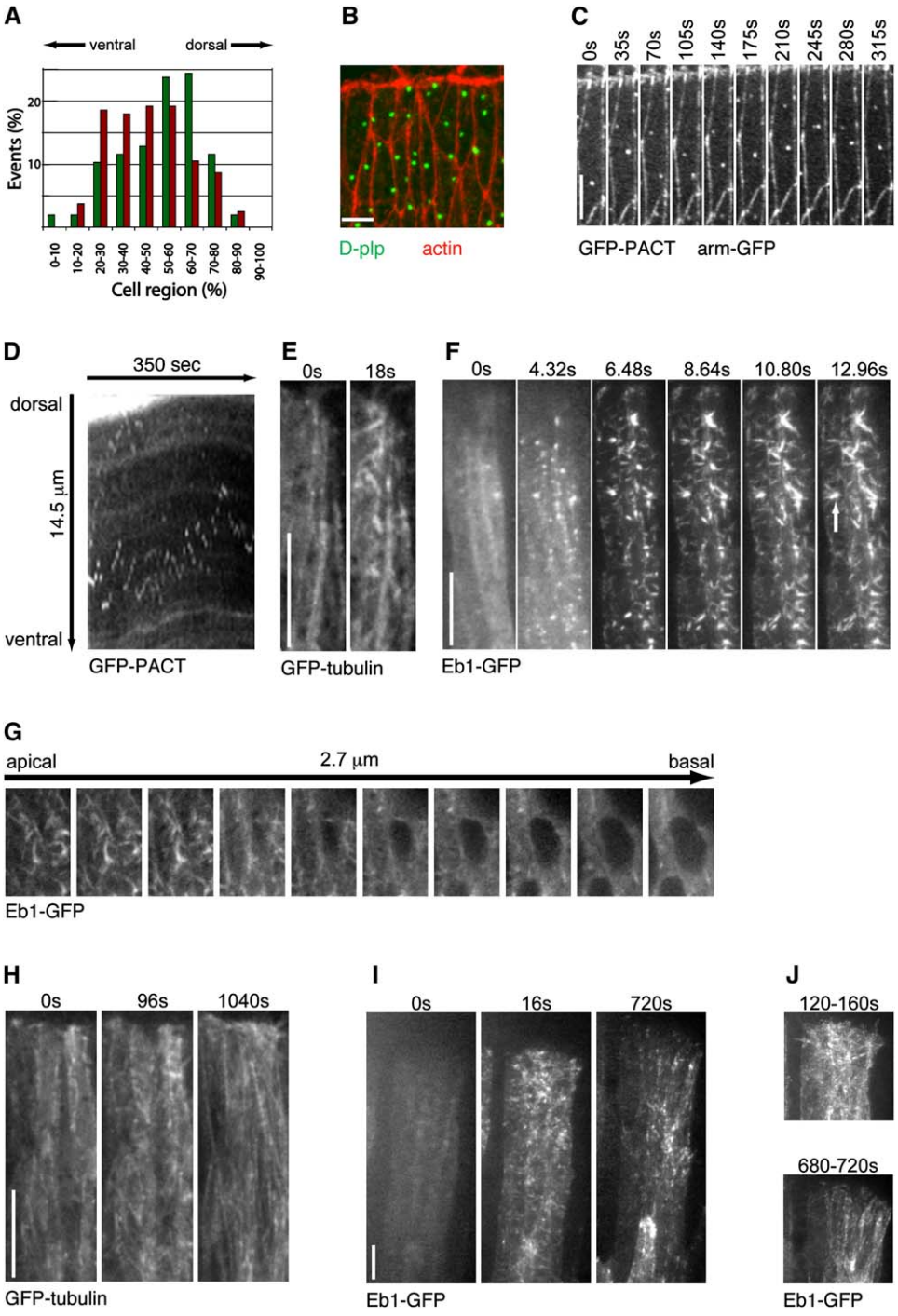

Figure 7. MT Minus Ends in DME Cells

Scale bars are 5 μm. (A) Graph showing the spatial distribution of EB1-GFP dot appearance and their subsequent direction of movement. Six cells from two embryos were divided into ten parts along the dorsal-ventral axis (0 = ventral, 100 = dorsal). Red bars represent EB1-GFP dots moving dorsally (n = 157), green bars ventrally moving dots (n = 164). (B) Immunofluorescence staining of a zippering-stage embryo with D-plp-L antibody (green) to visualize centrioles and phalloidin (red) to visualize actin and outline cells. (C) Movie sequence of a DME cell expressing GFP-PACT to visualize the centriole and Arm-GFP to outline the cell. (D) Kymograph of D/V centriole movement in the cell shown in (C). (E–I) Movie sequences of colcemid-injected embryos showing MT regrowth after UV-inactivation of colcemid. (E and F) Two second UV irradiation (between first and second frame). (E) Cells expressing GFP-tubulin. (F) Cells expressing EB1-GFP. The arrow depicts an MT aster. (G) Confocal sections of EB1-GFP-expressing DME cells immediately after UV-irradiation. (H and I) Fifteen second UV irradiation (between first and second frame). (H) GFP-tubulin-expressing cells. (I) EB1-GFP-expressing cells. (J) Projections of the first and last 20 consecutive time points of the movie sequence in (I).

the D/V cell axis within that time (Figures 7I and 7J and Movie S14). In the cylindrical fission yeast cells, a similar organization of MT bundles, parallel to the long cell axis occurs because the growing plus ends of misaligned MTs become deflected when they encounter the cell cortex in the cell center (Brunner and Nurse, 2000). However, in our experiments, we could not detect reorienting MTs. Instead, a subset of properly oriented MTs or MT bundles became more and more prominent, whereas misaligned MTs disappeared. This MT behavior was also reflected in the behavior of the EB1-GFP dots. These did not significantly change their direction of movement as would be expected if they were deflected. Instead, more and more of the newly appearing dots already started moving with the correct orientation. This suggests that the D/V orientation of MT bundles is not based on a simple deflection mechanism as in fission yeast.

Discussion

MT reorganization in nondividing cells occurs during developmental differentiation processes or if cells react to environmental changes for example after wounding of a tissue. The reason for such MT reorganization is often not known. In vivo studies of MT reorganization events in cells of multicellular organisms were mostly limited to large, autonomously functioning cells such as oocytes or to cultured cells or cell layers. Here, we show that *Drosophila* epithelial cells during DC represent an excellent experimental system, which provides sufficient subcellular resolution for the in vivo study of the nature and function of a transient MT reorganization event. Using time-lapse imaging of DC-stage embryos expressing GFP-tagged forms of tubulin or the plus end tracking protein EB1, we show that during DC, antiparallel MTs form stable bundles that align parallel to the D/V cell axis at the apical cell cortex. Within bundles, the MTs remain highly dynamic, which allows them to grow into the cellular protrusions that form at the dorsal surface of the DME cells. Surprisingly, elimination of these MTs by injection of MT depolymerizing drugs into the embryo or by expressing an MT-severing protein in a subset of epithelial cells inhibited exclusively the zippering process that completes DC. All other essential processes, the convergence of the two lateral epithelial cell layers, D/V cell polarization of the DMEs, or their actin-based dorsal constriction were not altered.

How could MT function be linked to zippering at the molecular level? One obvious scenario is that MTs are required for the local delivery of adhesion proteins. MT-based, localized delivery of factors was already shown to be crucial for proper morphogenesis in fission yeast cells and for a number of processes during early *Drosophila* development (Mata and Nurse, 1997; Theurkauf et al., 1992; Welte et al., 1998; Wilkie and Davis, 2001). However, zippering is not a simple one-step process. It is proposed to start with the interdigitation of the cell protrusions that form at the dorsal side of the DME cells and that establish the first contacts between equivalent cells of the two opposing epithelial cell layers (Jacinto et al., 2000). Consistent with this, the protrusions are essential for zippering (Homsy et al., 2006; Jacinto et al., 2000; Woolner et al., 2005). The initial cell-cell contacts subsequently develop into the known cell-adhesion structures. The possibility for initial interdigitation occurs at the anterior and posterior ends of the dorsal opening where the two cell layers meet. As this possibility also exists in embryos that cannot zipper due to a lack of MTs, it is conceivable that MTs are required for the interdigitation of protrusions. Intriguingly, the absence of MTs considerably affects the number and appearance of cellular protrusions known to be essential for zippering, which provides another possible explanation for the inability of these cells to interact with each other. An MT-mediated increase in protrusion formation could provide DME cells with sufficient interactive surface or interaction time to enable interdigitation. Consistent with this, the stripes of cells lacking MTs in our Spastin-overexpression experiments were unable to zipper on their own but eventually managed to establish cell adhesion when forced into close proximity by zippering of the neighboring wild-type cells. To understand MT function during zippering, one may therefore need to ask how MTs modify cell protrusions. As protrusions can still form in the absence of MTs, these do not seem to control the on/off activity of the protrusion-forming machinery but may rather modulate its activity. MTs were previously shown to affect protrusion formation in several cultured cell types but the molecular mechanisms are not clear (Etienne-Manneville and Hall, 2001; Gibney and Zheng, 2003; Liao et al., 1995; Rodionov et al., 1993; Waterman-Storer et al., 1999). It was speculated that MTs may modulate the actin machinery by delivering regulatory factors such as guanine nucleotide exchange factors or GTPase-activating proteins that modulate the actin organizing activities of the Rac1, Cdc42, and Rho GTPases (Glaven et al., 1999; Nalbant et al., 2004; Ren et al., 1998; Rogers et al., 2004). It is also possible that growing MTs produce pushing forces that support protrusion growth (Etienne-Manneville, 2004).

Why do MTs reorganize in such a specific way? We are unable to answer this question. If delivery of adhesion factors or promoting protrusion formation were indeed the critical functions of MTs, then their orientation parallel to the D/V cell axis would certainly improve delivery to the relevant site. However, because of the antiparallel arrangement, transport of factors is bidirectional, and therefore the factors would also be delivered to the wrong cell ends. In addition, MTs reorganize in all epithelial cells, although most of them are not involved in zippering and therefore do not need delivery of the proposed factors. It is possible that MTs reorganize to fulfill additional, nonessential functions that optimize the DC process. For example, we show that the MTs are required for proper epithelial cell morphology. During convergence, these cells gradually elongate along the D/V axis while thinning out in the apical-basal direction. Elongation coincides with the D/V alignment of the MTs, implying that MT reorganization may be the consequence of cell shape changes. However, cells lacking MTs cannot maintain their shape after an initial elongation phase, suggesting that proper cell morphology is dependent on MT function. Notably, this is not the consequence of defects in polarization, since cell polarity is not affected in the absence of MTs. The role of epithelial cell shape changes in DC is not clear. Their

dorsalward stretching may contribute to gap closure, but recent data indicated that it is not essential (Hutson et al., 2003). The finding that the shape abnormalities resulting from MT depletion did not affect convergence of epithelial cell layers is consistent with this view.

Our results provide further evidence that MT reorganization is not only crucial when cells change from an interphase to a mitotic state but also when they change behavior during development. It is important to understand how such rearrangements are controlled at the molecular level and also how cell-type-specific differences are achieved. DC in *Drosophila* provides an excellent experimental system in which the molecular mechanisms controlling MT organization can be studied in vivo by live imaging with appropriate subcellular resolution in combination with classical genetics.

Experimental Procedures

Cloning

EB1 fusion proteins were generated carrying an ILGAPSGGGATA GAGGAGGPAGLI linker sequence between EB1 and GFP. The linker-EYFP and linker-GFP fragments were excised BamHI/BglII from the plasmids pFA6A-LGFP-kanMX6 and pFA6A-LEYFP-kanMX6 (B. Hülsmann and D. Brunner, unpublished data) and cloned into the EcoRI/BglII cleaved pUAST vector together with PCR-amplified EcoRI-EB1-BamHI sequence (from LD08743 EST cDNA), generating pUAST-EB1-GFP and pUAST-EB1-EYFP. EB1-GFP and EB1-EYFP coding sequences were cloned EcoRI/XbaI into pUASP2 (Rorth, 1998). Transgenic *Drosophila* lines were generated by standard methods.

Immunohistochemistry

Embryos were dechorionated in 50% bleach and fixed for 40 min in heptane saturated with formaldehyde. Embryos were devitellinized by hand with a needle and incubated overnight at 4°C with primary antibodies in PBT-BSA (PBS, 0.1% Triton X-100, 0.5% BSA). Primary antibodies used: anti-Tubulin (1:100, Sigma), anti-plp-L (1:200, kind gift from J. Raff), anti-Dlg (1:20, Developmental Studies Hybridoma Bank). Secondary antibodies used: Alexa-488, Alexa-546 (1:1000 in PBT-BSA, Molecular Probes). To stain actin, embryos were incubated for 2 hr in rhodamin-phalloidin (2 unit/ml in PBT, Molecular Probes). Specimens were mounted in 50% glycerol/PBT and examined with Zeiss LSM 510 FCS or Olympus FW1000 confocal microscopes.

Fly Strains

Constructs used: GFP-tubulin (Grieder et al., 2000), Actin-EGFP (Fulga and Rorth, 2002), Actin-ECFP (Van Roessel et al., 2002), Fz-GFP (Strutt, 2001), Dlg-GFP (Koh et al., 1999), Arm-EGFP (McCartney et al., 2001), GFP-PACT (Martinez-Campos et al., 2004), Spastin-EGFP (Trotta et al., 2004), Moe-GFP (=sGMCA:GFP [Kiehart et al., 2000]), EB1-GFP, EB1-EYFP. MT imaging was done with homozygous UAS-GFP-tubulin;69B-Gal4 embryos. Actin and MTs were imaged simultaneously in 112A-Gal4/+;UAS-Actin-ECFP/UAS-GFP-tubulin;69B-Gal4/+ embryos. MTs and EB1 were imaged simultaneously in UAS-GFP-tubulin/UAS-EB1-EYFP;69B-Gal4/69B-Gal4 embryos. Spastin-overexpression imaging was done in Moe-EGFP/en-Gal4;UAS-Spastin-EGFP/+ embryos.

Live Imaging and Image Analysis

Embryos were dechorionated in 50% bleach, mounted in Halocarbon oil (Sigma) onto a glass bottom culture dish (MatTek), and imaged with an UltraView RS spinning disk confocal microscope (Perkin Elmer, Zeiss Axioscope). Projections and time-lapse series assembly were done with ImageJ; Kymographs with MetaMorph software. Simultaneous imaging of GFP-tubulin and EB1-EYFP was done on a Leica SP2 FCS confocal microscope. FRAP and iFRAP experiments were done on a Zeiss LSM 510 FCS microscope and analyzed as described in (Rabut and Ellenberg, 2005). To correct bleed-through between emission spectra (e.g., GFP and CFP or YFP), we used spectral unmixing and ImageJ as described (Zimmermann et al., 2003).

Embryos were injected anteriorly with colcemid (10 μg/ml in PBS) with femtotip needles (Eppendorf). The zippering phenotype was quantified from buffer- or colcemid-injected Moe-GFP or en-Gal4/+; UAS-Spas-EGFP/Moe-GFP embryos (n = 2, 4, 3) by measuring gap height and width. Amnioserosa dynamics were quantified by measuring the surface area of ten cells in synchronized, colcemid injected, Arm-EGFP expressing embryos.

Protrusions were quantified on synchronized buffer- or colcemid-injected en-Gal4/Actin-EGFP or en-Gal4/UAS-Actin-EGFP;UAS-Spas-EGFP embryos (n = 4, 4, 3). The lamellipodia surface of an entire En-expressing cell stripe was measured every five minutes (n = 15, 22, 9). The number of filopodia extending per minute was calculated from measurements in En stripes (n = 13, 13, 14) over more than 30 min. Geometric parameters were measured with ImageJ, numerical data were plotted with Microsoft Excel, and curve fitting was done with DataFit.

Supplemental Data

Supplemental Data include supporting movies and figures and are available at http://www.developmentalcell.com/cgi/content/full/11/3/375/DC1/.

Acknowledgments

We thank N. Grieder, P. Rorth, A. Brand, M. Peifer, D. Strutt, V. Budnik, J. Raff, A. Daga, D. Kiehart, Y. Zheng, and C. Himburg for fly stocks and reagents. We also thank Pernille Rorth, Lindsay Murrells, and Darren Gilmour for critical reading of the manuscript and the members of the Advanced Light Microscopy Facility for help with microscopy. F.J. was supported by a European Molecular Biology Organisation fellowship and in part by an Human Frontiers Science Program research grant.

Received: April 9, 2006
Revised: July 21, 2006
Accepted: July 26, 2006
Published: September 1, 2006

References

Akhmanova, A., and Hoogenraad, C.C. (2005). Microtubule plus-end-tracking proteins: mechanisms and functions. Curr. Opin. Cell Biol. *17*, 47–54.

Berdnik, D., and Knoblich, J.A. (2002). *Drosophila* Aurora-A is required for centrosome maturation and actin-dependent asymmetric protein localization during mitosis. Curr. Biol. *12*, 640–647.

Brunner, D., and Nurse, P. (2000). CLIP170-like tip1p spatially organizes microtubular dynamics in fission yeast. Cell *102*, 695–704.

Buck, K.B., and Zheng, J.Q. (2002). Growth cone turning induced by direct local modification of microtubule dynamics. J. Neurosci. *22*, 9358–9367.

Carazo-Salas, R.E., Antony, C., and Nurse, P. (2005). The kinesin Klp2 mediates polarization of interphase microtubules in fission yeast. Science *309*, 297–300.

Dammermann, A., Desai, A., and Oegema, K. (2003). The minus end in sight. Curr. Biol. *13*, R614–R624.

Desai, A., and Mitchison, T.J. (1997). Microtubule polymerization dynamics. Annu. Rev. Cell Dev. Biol. *13*, 83–117.

Dogterom, M., Kerssemakers, J.W., Romet-Lemonne, G., and Janson, M.E. (2005). Force generation by dynamic microtubules. Curr. Opin. Cell Biol. *17*, 67–74.

Edwards, K.A., Demsky, M., Montague, R.A., Weymouth, N., and Kiehart, D.P. (1997). GFP-moesin illuminates actin cytoskeleton dynamics in living tissue and demonstrates cell shape changes during morphogenesis in *Drosophila*. Dev. Biol. *191*, 103–117.

Etienne-Manneville, S. (2004). Actin and microtubules in cell motility: which one is in control? Traffic *5*, 470–477.

Etienne-Manneville, S., and Hall, A. (2001). Integrin-mediated activation of Cdc42 controls cell polarity in migrating astrocytes through PKCzeta. Cell *106*, 489–498.

Fulga, T.A., and Rorth, P. (2002). Invasive cell migration is initiated by guided growth of long cellular extensions. Nat. Cell Biol. *4*, 715–719.

Gibney, J., and Zheng, J.Q. (2003). Cytoskeletal dynamics underlying collateral membrane protrusions induced by neurotrophins in cultured *Xenopus* embryonic neurons. J. Neurobiol. *54*, 393–405.

Glaven, J.A., Whitehead, I., Bagrodia, S., Kay, R., and Cerione, R.A. (1999). The Dbl-related protein, Lfc, localizes to microtubules and mediates the activation of Rac signaling pathways in cells. J. Biol. Chem. *274*, 2279–2285.

Grieder, N.C., de Cuevas, M., and Spradling, A.C. (2000). The fusome organizes the microtubule network during oocyte differentiation in *Drosophila*. Development *127*, 4253–4264.

Grill, S.W., Gonczy, P., Stelzer, E.H., and Hyman, A.A. (2001). Polarity controls forces governing asymmetric spindle positioning in the *Caenorhabditis elegans* embryo. Nature *409*, 630–633.

Harden, N., Lee, J., Loh, H.Y., Ong, Y.M., Tan, I., Leung, T., Manser, E., and Lim, L. (1996). A *Drosophila* homolog of the Rac- and Cdc42-activated serine/threonine kinase PAK is a potential focal adhesion and focal complex protein that colocalizes with dynamic actin structures. Mol. Cell. Biol. *16*, 1896–1908.

Homsy, J.G., Jasper, H., Peralta, X.G., Wu, H., Kiehart, D.P., and Bohmann, D. (2006). JNK signaling coordinates integrin and actin functions during *Drosophila* embryogenesis. Dev. Dyn. *235*, 427–434.

Hutson, M.S., Tokutake, Y., Chang, M.S., Bloor, J.W., Venakides, S., Kiehart, D.P., and Edwards, G.S. (2003). Forces for morphogenesis investigated with laser microsurgery and quantitative modeling. Science *300*, 145–149.

Jacinto, A., Wood, W., Balayo, T., Turmaine, M., Martinez-Arias, A., and Martin, P. (2000). Dynamic actin-based epithelial adhesion and cell matching during *Drosophila* dorsal closure. Curr. Biol. *10*, 1420–1426.

Jacinto, A., Martinez-Arias, A., and Martin, P. (2001). Mechanisms of epithelial fusion and repair. Nat. Cell Biol. *3*, E117–E123.

Jacinto, A., Woolner, S., and Martin, P. (2002). Dynamic analysis of dorsal closure in *Drosophila*: from genetics to cell biology. Dev. Cell *3*, 9–19.

Kaltschmidt, J.A., Lawrence, N., Morel, V., Balayo, T., Fernandez, B.G., Pelissier, A., Jacinto, A., and Martinez Arias, A. (2002). Planar polarity and actin dynamics in the epidermis of *Drosophila*. Nat. Cell Biol. *4*, 937–944.

Karsenti, E., and Vernos, I. (2001). The mitotic spindle: a self-made machine. Science *294*, 543–547.

Kiehart, D.P., Galbraith, C.G., Edwards, K.A., Rickoll, W.L., and Montague, R.A. (2000). Multiple forces contribute to cell sheet morphogenesis for dorsal closure in *Drosophila*. J. Cell Biol. *149*, 471–490.

Koh, Y.H., Popova, E., Thomas, U., Griffith, L.C., and Budnik, V. (1999). Regulation of DLG localization at synapses by CaMKII-dependent phosphorylation. Cell *98*, 353–363.

Liao, G., Nagasaki, T., and Gundersen, G.G. (1995). Low concentrations of nocodazole interfere with fibroblast locomotion without significantly affecting microtubule level: implications for the role of dynamic microtubules in cell locomotion. J. Cell Sci. *108*, 3473–3483.

Martinez-Campos, M., Basto, R., Baker, J., Kernan, M., and Raff, J.W. (2004). The *Drosophila* pericentrin-like protein is essential for cilia/flagella function, but appears to be dispensable for mitosis. J. Cell Biol. *165*, 673–683.

Mata, J., and Nurse, P. (1997). tea1 and the microtubular cytoskeleton are important for generating global spatial order within the fission yeast cell. Cell *89*, 939–949.

McCartney, B.M., McEwen, D.G., Grevengoed, E., Maddox, P., Bejsovec, A., and Peifer, M. (2001). *Drosophila* APC2 and Armadillo participate in tethering mitotic spindles to cortical actin. Nat. Cell Biol. *3*, 933–938.

Megraw, T.L., Kilaru, S., Turner, F.R., and Kaufman, T.C. (2002). The centrosome is a dynamic structure that ejects PCM flares. J. Cell Sci. *115*, 4707–4718.

Mennella, V., Rogers, G.C., Rogers, S.L., Buster, D.W., Vale, R.D., and Sharp, D.J. (2005). Functionally distinct kinesin-13 family members cooperate to regulate microtubule dynamics during interphase. Nat. Cell Biol. *7*, 235–245.

Morel, V., and Arias, A.M. (2004). Armadillo/beta-catenin-dependent Wnt signalling is required for the polarisation of epidermal cells during dorsal closure in *Drosophila*. Development *131*, 3273–3283.

Nalbant, P., Hodgson, L., Kraynov, V., Toutchkine, A., and Hahn, K.M. (2004). Activation of endogenous Cdc42 visualized in living cells. Science *305*, 1615–1619.

Pizon, V., Gerbal, F., Diaz, C.C., and Karsenti, E. (2005). Microtubule-dependent transport and organization of sarcomeric myosin during skeletal muscle differentiation. EMBO J. *24*, 3781–3792.

Rabut, G., and Ellenberg, J. (2005). Photobleaching techniques to study mobility and molecular dynamics of proteins in live cells: FRAP, iFRAP and FLIP. In Live Cell Imaging: A Laboratory Manual, Volume One, R.D. Goldman and D.L. Spector, eds. (Cold Spring Harbor, NY: Cold Spring Harbor Laboratory Press), pp. 101–127.

Ren, Y., Li, R., Zheng, Y., and Busch, H. (1998). Cloning and characterization of GEF-H1, a microtubule-associated guanine nucleotide exchange factor for Rac and Rho GTPases. J. Biol. Chem. *273*, 34954–34960.

Riechmann, V., and Ephrussi, A. (2001). Axis formation during *Drosophila* oogenesis. Curr. Opin. Genet. Dev. *11*, 374–383.

Rodionov, V.I., Gyoeva, F.K., Tanaka, E., Bershadsky, A.D., Vasiliev, J.M., and Gelfand, V.I. (1993). Microtubule-dependent control of cell shape and pseudopodial activity is inhibited by the antibody to kinesin motor domain. J. Cell Biol. *123*, 1811–1820.

Rogers, S.L., Rogers, G.C., Sharp, D.J., and Vale, R.D. (2002). *Drosophila* EB1 is important for proper assembly, dynamics, and positioning of the mitotic spindle. J. Cell Biol. *158*, 873–884.

Rogers, S.L., Wiedemann, U., Hacker, U., Turck, C., and Vale, R.D. (2004). *Drosophila* RhoGEF2 associates with microtubule plus ends in an EB1-dependent manner. Curr. Biol. *14*, 1827–1833.

Rorth, P. (1998). Gal4 in the *Drosophila* female germline. Mech. Dev. *78*, 113–118.

Sherwood, N.T., Sun, Q., Xue, M., Zhang, B., and Zinn, K. (2004). *Drosophila* spastin regulates synaptic microtubule networks and is required for normal motor function. PLoS Biol. *2*, e429.

Strutt, D.I. (2001). Asymmetric localization of frizzled and the establishment of cell polarity in the *Drosophila* wing. Mol. Cell *7*, 367–375.

Theurkauf, W.E., Smiley, S., Wong, M.L., and Alberts, B.M. (1992). Reorganization of the cytoskeleton during *Drosophila* oogenesis: implications for axis specification and intercellular transport. Development *115*, 923–936.

Tran, P.T., Marsh, L., Doye, V., Inoue, S., and Chang, F. (2001). A mechanism for nuclear positioning in fission yeast based on microtubule pushing. J. Cell Biol. *153*, 397–411.

Trotta, N., Orso, G., Rossetto, M.G., Daga, A., and Broadie, K. (2004). The hereditary spastic paraplegia gene, spastin, regulates microtubule stability to modulate synaptic structure and function. Curr. Biol. *14*, 1135–1147.

Van Roessel, P., Hayward, N.M., Barros, C.S., and Brand, A.H. (2002). Two-color GFP imaging demonstrates cell-autonomy of GAL4-driven RNA interference in *Drosophila*. Genesis *34*, 170–173.

Waterman-Storer, C.M., Worthylake, R.A., Liu, B.P., Burridge, K., and Salmon, E.D. (1999). Microtubule growth activates Rac1 to promote lamellipodial protrusion in fibroblasts. Nat. Cell Biol. *1*, 45–50.

Welte, M.A. (2004). Bidirectional transport along microtubules. Curr. Biol. *14*, R525–R537.

Welte, M.A., Gross, S.P., Postner, M., Block, S.M., and Wieschaus, E.F. (1998). Developmental regulation of vesicle transport in *Drosophila* embryos: forces and kinetics. Cell *92*, 547–557.

Wilkie, G.S., and Davis, I. (2001). *Drosophila* wingless and pair-rule transcripts localize apically by dynein-mediated transport of RNA particles. Cell *105*, 209–219.

Woolner, S., Jacinto, A., and Martin, P. (2005). The small GTPase Rac plays multiple roles in epithelial sheet fusion—dynamic studies of *Drosophila* dorsal closure. Dev. Biol. *282*, 163–173.

Zimmermann, T., Rietdorf, J., and Pepperkok, R. (2003). Spectral imaging and its applications in live cell microscopy. FEBS Lett. *546*, 87–92.